

## Charge Correlations and Dynamical Instabilities in the Multifragment Emission Process

L. G. Moretto, Th. Rubehn, L. Phair, N. Colonna,\* and G. J. Wozniak

*Nuclear Science Division, Lawrence Berkeley National Laboratory, Berkeley, California 94720*

D. R. Bowman,<sup>†</sup> G. F. Peaslee,<sup>‡</sup> N. Carlin,<sup>§</sup> R. T. de Souza,<sup>||</sup> C. K. Gelbke, W. G. Gong,<sup>¶</sup> Y. D. Kim,<sup>\*\*</sup> M. A. Lisa,<sup>††</sup>  
W. G. Lynch, and C. Williams

*National Superconducting Cyclotron Laboratory and Department of Physics and Astronomy,  
Michigan State University, East Lansing, Michigan 48824*

(Received 26 March 1996)

A new, sensitive method allows one to search for the enhancement of events with nearly equal-sized fragments as predicted by theoretical calculations based on volume or surface instabilities. Simulations have been performed to investigate the sensitivity of the procedure. Experimentally, charge correlations of intermediate mass fragments emitted from heavy ion reactions at intermediate energies have been studied. No evidence for a preferred breakup into equal-sized fragments has been found. [S0031-9007(96)01258-6]

PACS numbers: 25.70.Pq, 24.10.Lx

In recent years, multifragmentation of nuclear systems has been extensively studied, and many efforts have been made to clarify the underlying physics [1]. It has been suggested that fragment production can be related to the occurrence of instabilities in the intermediate system produced by heavy ion collisions [2–13]. In particular, two kinds of instabilities are extensively discussed in the literature: volume instabilities of a spinodal type (see, e.g., Ref. [12]) and surface instabilities [3]. Spinodal instabilities are associated with the transit of a homogeneous fluid across a domain of negative pressure, where the homogeneous fluid becomes unstable and breaks up into droplets of denser liquid. Surface instabilities can be subdivided into Rayleigh or cylinder instabilities which are responsible for the decay of shapes like long necks or toroids [2], and sheet instabilities which cause the decay of bubbles or disklike structures [3]. Many models predict the formation of these exotic geometries which may develop after the initial compression of nuclei in the early stage of the collision for both symmetric and asymmetric systems [3,4,6,7,10–13]. Although the scenarios and the models vary, breakup into several *nearly equal-sized* fragments has been discussed for both kinds of instabilities [14]. In this Letter, we examine model independent signatures that would indicate decay into a number of nearly equal-sized fragments by investigating charge correlations from both experimental data and simulations.

We have experimentally studied the reactions Xe + Cu at  $E/A = 50$  MeV. The measurements were performed at the National Superconducting Cyclotron Laboratory of Michigan State University using the Miniball [15] and a Si-Si(Li)-plastic forward array [16]. Detailed information on the experiment can be found in Ref. [17].

For comparison, and to determine the sensitivity of our analysis, Monte Carlo calculations have been performed.

The created events obey two conditions: The sum charge of all fragments is conserved within an adjustable accuracy, and a fragment is produced according to the probability resulting from the experimental finding, that the charge distributions for  $n$  intermediate mass fragments (IMF:  $Z = 3-20$ ) are nearly exponential functions [18]:

$$P_n(Z) \propto \exp(-\alpha_n Z). \quad (1)$$

Experimentally, a variation of the parameter  $\alpha_n$  between 0.2 and 0.4 has been reported for extreme cuts on the transverse energy  $E_t$  (defined as  $\sum_i E_i \sin^2 \theta_i$ ) [17,19]. In our simulations, we have chosen  $\alpha_n = 0.3$  (different values between 0.2 and 0.4 do not change our findings). The size of the decaying source ( $Z_{\text{source}} = 83$ ) was chosen to be equal to the sum charge of Xe and Cu. Events with  $N_{\text{IMF}}$  equal sized fragments of charge  $Z_{\text{art}}$  were randomly added with probability  $P$  to simulate a dynamical breakup of the system into nearly equal-sized pieces. Furthermore, the charge distributions of the individual fragments of such an event were smeared out according to a Gaussian distribution. This smearing of the charge distribution accounts not only for the width of the distribution due to the formation process *per se*, but also for the probable sequential decay of the primary fragments (i.e., the evaporation of light charged particles). In the following, the full width at half maximum of this distribution is denoted by  $\omega$ . We have demanded that at least 75% of the total available charge is emitted according to Eq. (1); i.e., the production of particles was stopped in the simulation once this percentage had been reached. We note that in this simple approach the transverse energy  $E_t$  has not been simulated. Furthermore, we restrict our analysis to IMFs only.

First, we investigate two particle correlations. Both the experimental and the simulated events have been analyzed according to the following method. The two particle

charge correlations are defined by the expression

$$\frac{Y(Z_1, Z_2)}{Y'(Z_1, Z_2)} \Big|_{E_t, N_{\text{IMF}}} = C[1 + R(Z_1, Z_2)] \Big|_{E_t, N_{\text{IMF}}}. \quad (2)$$

Here,  $Y(Z_1, Z_2)$  is the coincidence yield of two particles of atomic number  $Z_1$  and  $Z_2$  in an event with  $N_{\text{IMF}}$  intermediate mass fragments and a transverse energy  $E_t$ . The background yield  $Y'(Z_1, Z_2)$  is constructed by mixing particle yields from different coincidence events selected by the same cuts on  $N_{\text{IMF}}$  and  $E_t$ . The normalization constant  $C$  ensures equal integrated yields of  $Y$  and  $CY'$ .

To demonstrate the sensitivity of our method to breakup configurations producing equal-sized fragments, we show in Fig. 1 the results of simulations for the case  $N_{\text{IMF}} = 6$ . Here, a ‘‘contamination’’ of 1% of the events consisting of fragments which all have the size  $Z_{\text{art}} = 6$  has been added to the data set. The peak produced by these fragments is clearly visible, even if we decrease the yield of equal-sized fragments to only 0.1%. A different choice of  $Z_{\text{art}}$  does not change our results; higher values would produce an even larger signal since the denominator value is smaller.

The magnitude of the peak shown in Fig. 1 depends not only on the yield, but also on the width of the charge distribution of the nearly equal-sized fragments. In Fig. 2, we show the correlation functions (solid circles) for different widths  $\omega$  and for  $Z_1 = 6$ . For comparison, we have plotted the results of a calculation (open circles) where no additional events with equal-sized fragments have been added: As expected, a dependence of the size of the peak on the smearing can be observed which limits the sensitivity of the two particle correlation functions to an enhancement of events where the charge distribution is relatively narrow. Thus, for possible secondary decay resulting in large values of  $\omega$ , our analysis might not be adequate. However, the narrow widths predicted in Ref. [7], should be visible in the experimental data. The same analysis used for the simulation has been applied to experimental data. In Fig. 3, we show the results for central collisions (top 5% of events sorted by  $E_t$ )

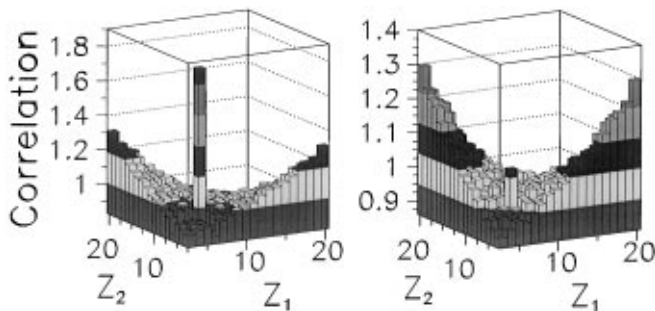


FIG. 1. Two particle charge correlations of IMFs from simulations investigating events with  $N_{\text{IMF}} = 6$  and a source size of 83. Randomly, 1% (left panel) and 0.1% (right panel) of the events were chosen to have equal sized fragments ( $Z_{\text{art}} = 6$ ).

of Xe + Cu at  $E/A = 50$  MeV for different  $N_{\text{IMF}}$  cuts. With higher fragment multiplicity the distribution peaked along the line  $Z_1 + Z_2 \approx 30$  changes into a distribution peaked at values where one fragment is heavy and its partner is light. However, an enhanced signal for breakup into nearly equal-sized fragments (a signal appearing along the diagonal) was not observed in *any* of the  $N_{\text{IMF}}$  bins. As an example, we show in Fig. 2 the experimental two particle correlation function vs  $Z_2$  for  $N_{\text{IMF}} = 6$  and  $Z_1 = 6$  (triangles).

Furthermore, we have investigated the correlation functions obtained by our simulations without enhanced breakup for several IMF multiplicities. The evolution of the shape of the distribution with increasing values of  $N_{\text{IMF}}$  is very similar to that observed in the experimental data of Fig. 3. Simulations with different system sizes show that the charge correlations decrease as  $Z_{\text{source}}$  increases; this can be attributed to the definition of an IMF ( $3 \leq Z_{\text{IMF}} \leq 20$ ) relative to  $Z_{\text{source}}$ . We have also performed calculations using a percolation code and have observed a dependence similar to that presented in Fig. 3. To further study the evolution of the distributions’ shape with multiplicity, we have investigated the breakup of an integer number  $Z_0$  (chain) into  $n$  pieces. The calculated two particle correlation functions for different multiplicities  $n$  have an evolution with  $n$  similar to that shown in Fig. 3. These findings suggest that the observed experimental evolution of the shape of the two particle charge correlation distribution with fragment multiplicity may be due to the limited number of possibilities to

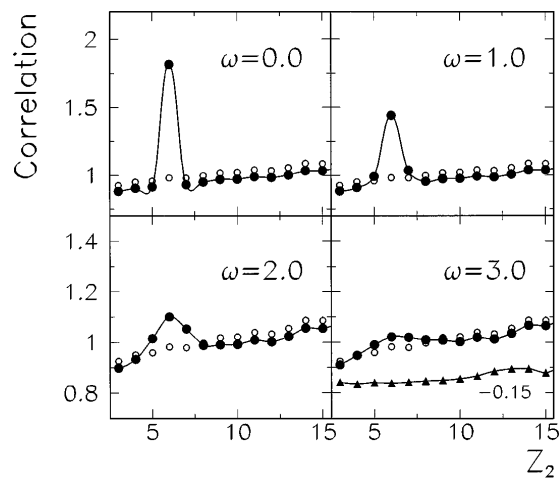


FIG. 2. Two particle charge correlations resulting from simulations for  $Z_1 = 6$  as a function of the fragment charge  $Z_2$  for different values of the width of the charge distribution  $\omega$ . Randomly, 1% of the events were chosen to have nearly equal sized fragments (full circles). For comparison, we have also plotted a calculation where no additional events with equal-sized fragments have been added (open circles). Experimental results for the case  $N_{\text{IMF}} = 6$  are shown in the right lower panel (full triangles). For clarity, these values are vertically shifted by a value of  $-0.15$ . The error bars are smaller than the size of the symbols.

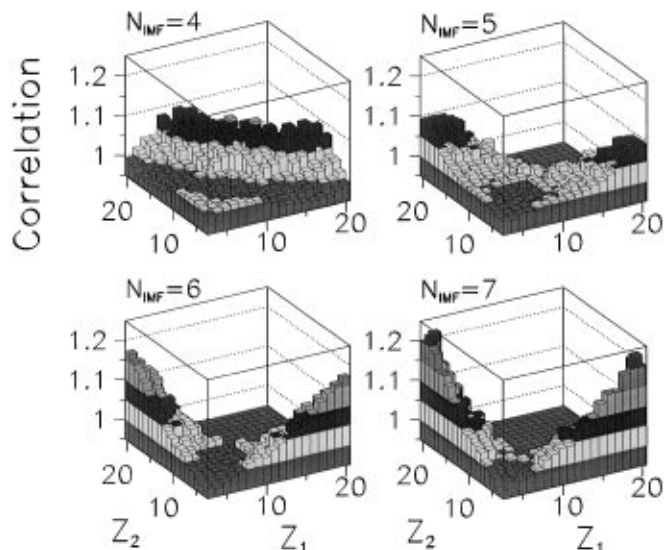


FIG. 3. Experimental two particle charge correlations for the reaction Xe + Cu at  $E/A = 50$  MeV. The different figures correspond to  $N_{\text{IMF}}$  cuts between 4 and 7.

create fragments if charge is conserved and the number of fragments is fixed. A signal of enhanced emission will sit on top of such a background.

Historically, charge correlations have often been investigated by using Dalitz plots [20,21]. However, this technique does not provide a sensitive tool to search for a weakly *enhanced* breakup into several nearly equal-sized fragments, since the “background” is ignored. The Dalitz analysis is equivalent to studying *only* the numerator of the charge correlation function and reflects mainly charge conservation instead of correlation enhancements of dynamical origin. Thus the strong signal shown in Fig. 1 does not show up in a Dalitz plot. Furthermore, the Dalitz plots and the charge distributions of the three largest fragments from Ref. [21], which are claimed to be a signature for an enhanced breakup into nearly equal-sized fragments, can be reproduced astonishingly well by our simple simulation. Thus these “signals” are almost completely dominated by the background produced by charge conservation.

To search for weak signals of events with nearly equal-sized fragments, and in the hope of increasing the sensitivity of the method, we have investigated higher order charge correlations [22]. This quantity is defined by the expression

$$\frac{Y(\Delta Z, \langle Z \rangle)}{Y'(\Delta Z, \langle Z \rangle)} \Bigg|_{E_i, N_{\text{IMF}}} = C[1 + R(\Delta Z, \langle Z \rangle)]_{E_i, N_{\text{IMF}}}. \quad (3)$$

Here,  $\langle Z \rangle$  denotes the average fragment charge of the event  $\langle Z \rangle = \sum_{i=1}^{N_{\text{IMF}}} Z_i / N_{\text{IMF}}$  and  $\Delta Z$  is the standard deviation, defined by  $\Delta Z = \sqrt{(N_{\text{IMF}} - 1)^{-1} \sum_{i=1}^{N_{\text{IMF}}} (Z_i - \langle Z \rangle)^2}$ . The normalization constant  $C$  and the yields are defined according

to Eq. (2). The denominator for the background yield  $Y'(\Delta Z, \langle Z \rangle)$  is obtained by constructing “pseudoevents” where one fragment is selected from each of the previous  $N_{\text{IMF}}$  events of the same event class (same  $E_i$  range).

In Fig. 4, we show the results of an analysis investigating higher order charge correlations. The same simulation which has already been shown in Fig. 1 was used. Here, only 0.1% of the events were chosen to have fragments with equal size. We show two cases with a width of  $\omega = 0$  and  $\omega = 2$ , respectively. The comparison between the two particle and the higher order charge correlation functions for the same simulations using  $\omega = 0$  shows an enhancement of  $\sim 20\%$  for the two particle correlation while the signal in the higher order correlation exceeds the “background” by roughly a factor of 100. Since the yield in the  $\Delta Z = 0$  bin increases dramatically with *any* enhancement of events with equal-sized fragments, it should be sufficient to examine this bin only; the correlations at higher values of  $\Delta Z$  represent the “background.”

We have analyzed our experimental data and determined the higher order charge correlation functions. The results are shown in Fig. 5 for the reaction Xe + Cu at  $50 E/A = \text{MeV}$ . For comparison, we also show the results of the simulation already shown in the right panel of Fig. 4 for  $N_{\text{IMF}} = 6$ ,  $P = 0.1\%$ , and  $\omega = 2$ . As discussed above, we compare the correlation values for  $\Delta Z = 0$  (solid symbols) with the data obtained for  $\Delta Z > 0$  (open symbols). No signals are observed that can be attributed to an enhanced production of nearly equal-sized fragments. This results in an upper limit of breakup events with nearly equal-sized fragments of less than 0.05% if we assume a width  $\omega < 3$ . Similar results have been obtained for the reactions Ar + Au at 50 and 110 MeV and Xe + Au at 50 MeV/nucleon [17,19] albeit with significantly poorer statistics. Thus the Xe + Cu system has been used to establish an upper limit for this system and to explore the utility of this novel technique.

In conclusion, we have investigated charge correlation functions of multifragment decays to search for the

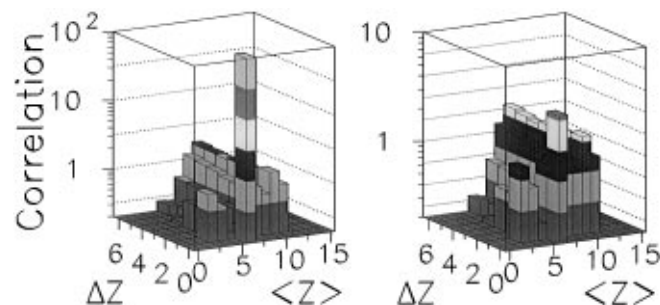


FIG. 4. Higher order charge correlations from the simulations for  $N_{\text{IMF}} = 6$ . Randomly, 0.1% of the events were chosen to have equal-sized fragments. Widths of  $\omega = 0$  (left panel) and  $\omega = 2$  are shown. Note the logarithmic scale of the correlation axis.

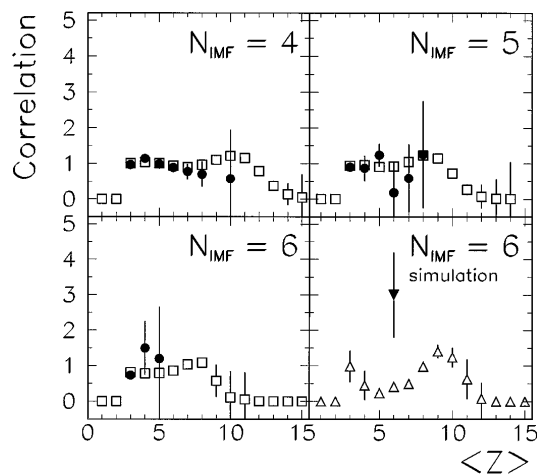


FIG. 5. Higher order charge correlations for the reaction Xe + Cu at  $E/A = 50$  MeV for  $4 \leq N_{IMF} \leq 6$ . For comparison, we show the results of the simulation for  $N_{IMF} = 6$  and  $\omega = 2$  (lower right panel). The full symbols indicate the events where  $\Delta Z = 0$ , the open symbols show the “background” defined by  $\Delta Z > 0$ .

enhanced production of nearly equal-sized fragments predicted in several theoretical works. Two particle charge correlation functions are sensitive to those enhancements from events where a number of equal-sized fragments might be accompanied by heavy partners, as could be expected from the breakup of a necklike structure. While the higher order charge correlations are not sensitive to necklike emission, they do provide an even more sensitive tool for identifying enhancements associated with the emission of all nearly equal-sized fragments. The analysis of experimental data for the reactions Xe + Cu and Xe + Cu at  $E/A = 50$  MeV and Ar + Au at  $E/A = 50$  and 110 MeV, however, shows no evidence for a preferred breakup into nearly equal-sized fragments. Recently, two groups have reported experimental signatures of possible formations of noncompact geometries in the reactions  $^{86}\text{Kr}$  on  $^{93}\text{Nb}$  at  $E/A = 65$  MeV and Pb + Au at  $E/A = 29$  MeV, respectively [23,24]. It would be interesting to analyze these data using the method presented in this Letter.

This work was supported by the Director, Office of Energy Research, Office of High Energy and Nuclear Physics, Nuclear Physics Division of the U.S. Department of Energy, under Contract No. DE-AC03-76SF00098 and by the National Science Foundation under Grants No. PHY-8913815, No. PHY-90117077, and No. PHY-9214992.

\*Present address: INFN-Sez. di Bari, 70126 Bari, Italy.

†Present address: Chalk River Laboratories, Chalk River, Ontario K0J 1J0, Canada.

‡Present address: Physics Department, Hope College, Holland, MI 49423.

§Present address: Instituto de Fisica, Universidade de Sao Paulo, C.P. 66318, CEP 04389-970, Sao Paulo, Brazil.

||Present address: Department of Chemistry, Indiana University, Bloomington, IN 47405.

¶Present address: Max-Planck-Institut für Physik, Föhringer Ring 6, 80805 München, Germany.

\*\*Present address: Physics Department, Seoul National University, Seoul, 151-742, Korea.

††Present address: Lawrence Berkeley National Laboratory, Berkeley, CA 94720.

- [1] L. G. Moretto and G. J. Wozniak, *Annu. Rev. Nucl. Part. Sci.* **43**, 379 (1993), and references therein.
- [2] U. Brosa, S. Grossmann, A. Müller, and E. Becker, *Nucl. Phys.* **A502**, 423c (1989); *Phys. Rep.* **197**, 167 (1990).
- [3] L. G. Moretto, K. Tso, N. Colonna, and G. J. Wozniak, *Nucl. Phys.* **A545**, 237c (1992); *Phys. Rev. Lett.* **69**, 1884 (1992).
- [4] W. Bauer, G. F. Bertsch, and H. Schulz, *Phys. Rev. Lett.* **69**, 1888 (1992).
- [5] D. H. E. Gross, B. A. Li, and A. R. DeAngelis, *Ann. Phys. (Leipzig)* **1**, 467 (1992).
- [6] S. R. Souza and C. Ngô, *Phys. Rev. C* **48**, R2555 (1993).
- [7] H. M. Xu *et al.*, *Phys. Rev. C* **48**, 933 (1993).
- [8] L. Phair, W. Bauer, and C. K. Gelbke, *Phys. Lett. B* **314**, 271 (1993).
- [9] T. Glasmacher, C. K. Gelbke, and S. Pratt, *Phys. Lett. B* **314**, 275 (1993).
- [10] B. Borderie, B. Remaud, M. F. Rivet, and F. Sebille, *Phys. Lett. B* **302**, 15 (1993).
- [11] S. Pal, S. K. Samaddar, A. Das, and J. N. De, *Phys. Lett. B* **337**, 14 (1994).
- [12] Ph. Chomaz, M. Colonna, A. Guanera, and B. Jacquot, *Nucl. Phys.* **A583**, 305c (1995).
- [13] D. O. Handzy *et al.*, *Phys. Rev. C* **51**, 2237 (1995).
- [14] M. Bruno *et al.*, *Phys. Lett. B* **292**, 251 (1992); *Nucl. Phys.* **A576**, 138 (1994).
- [15] R. T. de Souza *et al.*, *Nucl. Instrum. Methods Phys. Res., Sect. A* **311**, 109 (1992).
- [16] W. C. Kehoe *et al.*, *Nucl. Instrum. Methods Phys. Res., Sect. A* **311**, 258 (1992).
- [17] D. R. Bowman *et al.*, *Phys. Rev. C* **46**, 1834 (1992).
- [18] L. Phair *et al.*, *Phys. Rev. Lett.* **75**, 213 (1995).
- [19] L. Phair *et al.*, *Nucl. Phys.* **A564**, 453 (1993).
- [20] P. Kreuz *et al.*, *Nucl. Phys.* **A556**, 672 (1993).
- [21] A. Guarnera, Ph. Chomaz, and M. Colonna, in *Proceedings of the 34th International Winter Meeting on Nuclear Physics, Bormio, Italy, 1996*, edited by I. Iori (Ricerca Scientifica ed Educazione Permanente, to be published).
- [22] The term “higher order charge correlations” reflects the fact that all fragments of one event are taken into account.
- [23] N. T. B. Stone *et al.*, in *Proceedings of the 12th Winter Workshop on Nuclear Dynamics, Snowbird, Utah, 1996*, edited by W. Bauer and G. D. Westfall (Plenum, New York, to be published).
- [24] D. Durand *et al.*, *Phys. Lett. B* (to be published); J. F. Lecolley *et al.*, *Phys. Lett. B* (to be published).